

Sensitized Electroluminescence on Mesoporous Oxide Semiconductor Films[†]

Yordan Athanassov, François P. Rotzinger, Péter Péchy, and Michael Grätzel*

Institut de Chimie Physique, Ecole Polytechnique Fédérale de Lausanne, CH-1015 Lausanne, Switzerland

Received: July 18, 1996; In Final Form: October 7, 1996[⊗]

Forward biasing of a mesoporous TiO₂ (anatase) film whose surface is derivatized with a monolayer of the phosphonated ruthenium bipyridyl complex RuL₂L' with L = 4,7-diphenyl-1,10-phenanthroline and L' = 2,2'-bipyridine-4,4'-diphosphonic acid produces electroluminescence in the presence of an electrolyte containing peroxydisulfate in dimethylformamide. Light emission arises from the MLCT excited state of the complex which is generated directly through interfacial electron transfer from the conduction band of the semiconductor to the π* orbital of the oxidized Ru(III) state of RuL₂L'. The nanocrystalline morphology of the oxide film used here as electron injection electrode plays an important role in enhancing the electroluminescence process.

Introduction

Nanocrystalline semiconductors are the focus of many recent investigations.^{1–7} Mesoporous films of these materials are distinguished by a very high internal surface area, the roughness factor defined as the ratio between the real and projected surface of the film being about 1000 for an 8 μm thick layer. Pores in the nanometer size range are constituted by the voids present between the semiconductor particles. These are interconnected and are filled with an electrolyte or a solid conductor or semiconductor. Due to the very large internal surface area, these systems offer a number of intriguing features which have been exploited for the design of improved optoelectronic devices. Thus, dye sensitized mesoscopic oxide films have shown strikingly high photovoltaic conversion efficiencies.^{8–11} The transparent nature of these films allows for the direct monitoring of electron transfer processes by spectroscopic means. A new field for which the term “optical electrochemistry” has been coined is emerging from these investigations.^{12–14} TiO₂ has so far been the most studied material for nanocrystalline electrodes, but other materials have also been investigated, such as Fe₂O₃,¹⁵ ZnO,^{5,14} and CdSe/CdS³.

The investigation presented here takes advantage of the unique morphology of nanocrystalline semiconductor junctions to induce electroluminescence from a light emitting dye that is anchored as a monolayer through phosphonate groups to the surface of the oxide. It will be shown that the excited state of the dye is produced directly by interfacial electron transfer from the conduction band of the TiO₂ into the π* orbital of the diphenylphenanthroline ligand of RuL₂L', the Ru being promoted to the +III oxidation state through prior oxidation of the divalent complex by peroxydisulfate. The high surface area of the films enables this process to take place under mild accumulation conditions, where energy transfer quenching of the excited dye by the conduction band electrons present at the oxide surface is inefficient.

Experimental Section

Nanocrystalline Film Preparation. Nanocrystalline titanium dioxide was prepared by hydrolysis of titanium tetraisopropoxide as reported elsewhere.⁸ The only modification from the original procedure was that the autoclaving temperature was generally

210 or 230 °C instead of 200 °C. Spectroelectrochemical measurements employed transparent electrodes prepared by spreading the nanocrystalline TiO₂ autoclaved at 210 °C on a glass substrate coated with transparent conducting oxide (TCO), i.e., fluorine doped SnO₂. The TCO glass was obtained from Nippon Sheet Inc. (sheet resistance, 10 Ω/square; optical transmission, >80% in the visible). After air-drying, the electrode was fired for 30 min at 450 °C in air. The resulting film thickness was ca. 5 μm measured by profilometry. X-ray diffraction established that the colloidal TiO₂ film had 100% anatase crystal structure. SEM studies showed the film to be mesoporous from the outer layers to the TCO back contact with a relatively uniform particle size of 15 nm in diameter. Electro- and photoluminescence experiments employed titanium substrates (plates or rods of 0.5 cm diameter and 1.2 cm height) to support the nanocrystalline TiO₂. In this case the colloid was autoclaved at 230 °C. Prior to deposition of the TiO₂ paste, the titanium was cleaned by sonication in a detergent (Kieselgur) and a subsequent rinse with water. Prior to coating of the electrodes, Scotch tapes were applied in order to delimit the film area. The paste was then applied to the plate and spread by means of a glass cylinder. To coat the titanium rod, it was inserted in a perforated titanium sheet, the top of the rod being made coplanar with the plate. After spreading the paste, the electrode was withdrawn from the hole and allowed to dry in air at room temperature followed by annealing at 500 °C in an oxygen atmosphere for 30 min. The resulting film was again approximately 5 μm thick, and it was composed of particles with an average diameter of 20 nm.

The RuL₂L' was deposited onto the nanocrystalline TiO₂ film by overnight immersion of the electrode in a 2.5 × 10⁻⁵ M dye solution in a mixed solvent of dimethyl sulfoxide (DMSO) and EtOH (20/80, v/v). The volume of the liquid was adjusted to 5 mL/cm² of geometric electrode surface area. The apparent surface concentration of the dye measured by absorption spectroscopy was (2.1 ± 0.2) × 10⁻⁸ mol/cm². In order to ascertain that the dye remained anchored to the TiO₂ during the electrochemical experiments, the nanocrystalline electrode, after loading with RuL₂L' and rinsing with ethanol, was immersed overnight in 5 mL of electrolyte consisting of 100 mM tetrabutylammonium tetrafluoroborate ((TBA)BF₄) in dimethylformamide (DMF). At this time the dye concentration in the electrolyte determined by fluorescence analysis indicated that less than 1% of the RuL₂L' had desorbed after equilibration. One infers from this observation that the RuL₂L' is strongly and irreversibly attached to the mesoporous TiO₂ film. Dye

[†] In commemoration of the life and scientific achievements of Prof. Heinz Gerischer.

* Author to whom correspondence should be addressed.

[⊗] Abstract published in *Advance ACS Abstracts*, March 1, 1997.

uptake by the film was found to be limited to the amount corresponding to monolayer coverage, any $\text{RuL}_2\text{L}'$ in excess of this quantity remaining in solution. Moreover, the $\text{RuL}_2\text{L}'$ remained associated with the electrode even when the latter was held for several hours at -1.5 V, where reduction of the dye occurs. This distinguishes phosphonated bipyridyl complexes of ruthenium from carboxylated ones which often desorb from TiO_2 films upon reduction.

Materials. The ligand 2,2'-bipyridine-4,4'-bis(diethylphosphonate) was prepared, using an extension of the pyridine-3-phosphonic acid diethyl ester synthesis by Hirao et al.¹⁶, from 4,4'-dibromo-2,2'-bipyridine (0.47 g, 1.5 mmol, synthesized as described by Maerker and Case¹⁷) with palladium tetrakis-(triphenylphosphine) (0.18 g, 0.15 mmol), diethylphosphite (0.56 g, 4.1 mmol), and triethylamine (0.42 g, 4.15 mmol) measured into an argon filled flask, equipped with a cold finger and magnetic stirrer. Heated on a 98°C oil bath for 3 h, the reaction was monitored with TLC on silica gel plates: DCM:MeOH, 10:1; $R_f(1) = 0.64$. To the solidified mixture, cooled back to room temperature, dichloromethane:methanol was added (8 mL, 1:1), stirred for 10 min, and evaporated to dryness under reduced pressure. The residue was chromatographed on a silica gel column (gradient elution with DCM:MeOH), the fractions containing 2,2'-bipyridine-4,4'-bis(diethylphosphonate) were evaporated to dryness (0.27 g, 53% (corrected for the unreacted 4,4'-dibromo-2,2'-bipyridine)). From earlier fractions unreacted starting material was recovered (0.1 g). $^1\text{H-NMR}$ (200 MHz, CDCl_3): δ 1.36 (12H, t, 7 Hz), 4.20 (8H, m), 7.72 (2H, ddd, 14 Hz, 5 Hz, 1 Hz), 8.77 (2H, dt, 14 Hz, 1 Hz), 8.84 (2H, dt, 5 Hz, 1 Hz) ppm. $^{13}\text{C-NMR}$ (CDCl_3): δ 16.34 (d, $^3J_{\text{C-P}} = 5$ Hz), 62.79 (d, $^2J_{\text{C-P}} = 5$ Hz), 122.84 (d, $^2J_{\text{C-P}} = 9$ Hz), 125.65 (d, $^3J_{\text{C-P}} = 9$ Hz), 138.72 (d, $^1J_{\text{C-P}} = 186$ Hz), 149.58 (d, $^2J_{\text{C-P}} = 13$ Hz), 155.71 (d, $^3J_{\text{C-P}} = 14$ Hz) ppm. $^{31}\text{P-NMR}$ (CDCl_3): 15.06 ppm. MS (IC; m/z (rel intens): 429 (M + 1, 44.82), 428 (M⁺, 5.7), 386 (19.8), 355 (5.0), 335 (5.9), 321 (3.2), 320 (24.8), 314 (9.0), 305 (4.9), 292 (100), 291 (4.9), 281 (9.3), 264 (4.5), 248 (5.3), 236 (13.9), 218 (8.1), 217 (3.2), 216 (8.5), 211 (2.6), 188 (14.7), 176 (9.5), 157 (10.7), 151 (3.6), 147 (4.3), 109 (8.3), 98 (15.5). Anal. Calcd for $\text{C}_{18}\text{H}_{26}\text{N}_2\text{O}_6\text{P}_2$ (428.36): C, 50.47; H, 6.12; N, 6.54; P, 14.46%. Found: C, 50.67; H, 6.25; N, 6.69; P, 14.50%

The heteroleptic ruthenium complex $\text{RuL}_2\text{L}'$ (L = 4,7-diphenyl-1,10-phenanthroline and L' = 2,2'-bipyrid-4,4'-yl-diphosphonic acid) was produced in two steps: first the bisphenanthroline complex RuL_2Cl_2 was prepared followed by replacement of the chloride by the bipyridyldiphosphonic ester ligand. A 260 mg amount of commercial $\text{RuCl}_3 \cdot x\text{H}_2\text{O}$ (1.0 mmol) and 340 mg of LiCl (8 mmol) were dissolved in 20 mL of DMF. Then, 664 mg (2 mmol) of commercial 4,7-diphenyl-1,10-phenanthroline were added, and the mixture was refluxed under N_2 for 3 h. The solution was allowed to cool and stand for 18 h. Most of the DMF was then removed on the rotary evaporator, and the crude product was dissolved in 100 mL of hot EtOH to which was added slowly 100 mL of hot water containing 1–1.5 mL of concentrated HCl. The mixture was refluxed (10 min) and allowed to cool. The precipitate was collected by filtration and washed with 50 mL of EtOH:H₂O (1:1) containing 0.5 mL of concentrated HCl, and then with H₂O. This product was contaminated with $[\text{RuL}_3]\text{Cl}_2$. A $[\text{RuL}_3]\text{Cl}_2$ -free product was obtained by repeating the above procedure three times. This crude material is sufficiently pure for use in the subsequent step. A 167 mg amount of RuL_2Cl_2 (0.2 mmol), 90 mg of 2,2'-bipyrid-4,4'-yl-diphosphonic acid diethyl ester (0.21 mmol), and ca. 50 mg of triethylamine were refluxed for 7 h under N_2 in 10 mL of EtOH. The reaction mixture was

allowed to cool, and insoluble impurities were removed by filtration. After the addition of 7 mL of H₂O, the solution was refluxed for 5 h. Then, 7 mL of concentrated HCl was added, and the mixture was refluxed for 1 day. The EtOH was removed, the solution allowed to cool, and the product isolated by filtration and washed with H₂O. Finally, the product was refluxed for 2–3 h in acetone, filtered, and washed with acetone. This product is free (<1%) of RuL_3 , RuLL'_2 , and RuL'_3 on the basis of $^1\text{H-NMR}$ measurements. $^1\text{H-NMR}$ (400 MHz, CD_3OD): δ 7.60–7.76 (24H, m), 7.91 (2H, d, 5 Hz), 7.98 (2H, dd, 5 Hz, 5 Hz), 8.25 (2H, d, 5 Hz), 8.34 (4H, dd, 13.0 Hz, 10.0 Hz), 8.46 (2H, d, 5 Hz), 8.98 (2H, d, 13.0 Hz) ppm. $^{31}\text{P-NMR}$ (CD_3OD): δ 6.01 ppm. Anal. Calcd for $\text{C}_{58}\text{H}_{49}\text{Cl}_2\text{N}_6\text{O}_9.5\text{P}_2\text{-Ru}$ for $[\text{RuL}_2\text{L}']\text{Cl}_2 \cdot 3.5\text{H}_2\text{O}$: C, 57.29; H, 4.06; N, 6.91%. Found: C, 57.30; H, 4.15; N, 6.97%.

Methods. $^1\text{H-NMR}$ spectra were measured on BRUKER ACP-200 and BRUKER DPX-400 spectrometers at 200 MHz and 400 MHz: ^{31}P - and ^{13}C -NMR spectra were measured on the ACP-200 at 81.0 and 50.2 MHz, respectively. Chemical shifts are given in δ (ppm) relative to TMS (^1H , ^{13}C) and to 85% H_3PO_4 (^{31}P). Mass spectra (m/z relative percent) were measured with a Nermag-R-10-10C spectrometer. Electrochemical measurements used a three-electrode three-compartment setup. The rod electrodes were incorporated in a Teflon tube with an external diameter of 1 cm to obtain a rotating disk electrode. A silver wire quasi-reference electrode was used, but all potentials are given hereafter with respect to the Ag/AgCl saturated reference electrode. A platinum wire was used as counter electrode. The electrolyte consisted in most cases of a 0.1 M tetrabutylammonium tetrafluoroborate ((TBA)BF₄) solution in water-free *N,N*-dimethylformamide (DMF). They were purchased, as sodium peroxodisulfate and iodine, by Fluka, and used as received, except for (TBA)BF₄, which was dried for 5 h at 120°C under vacuum (10^{-2} Torr). 1-Hexyl-3-methylimidazolium iodide was synthesized as reported elsewhere.¹⁸ Current voltage curves were recorded using an EG&G Princeton Applied Research Model 362 or an Eco Chemie Autolab scanning potentiostat. Luminescence measurements were performed by placing the electrochemical cell in the compartment of a Spex F 112 fluorimeter equipped with a cooled Hamamatsu R 2658 photomultiplier tube mounted on the emission monochromator. The photomultiplier was configured for single photon counting. All spectra were corrected for the spectral sensitivity of the monochromator and the photomultiplier. A Balzers B-40 448 nm interference filter was used when the TiO_2 was deposited on a titanium plate. Absorption measurements were performed on a Varian Cary 1E UV-visible spectrophotometer. All measurements were performed at room temperature.

Results and Discussion

Figure 1 shows the luminescence and luminescence excitation spectrum of $\text{RuL}_2\text{L}'$ in DMF. The emission peaks at 650 nm, its quantum yield being about 8%. The feature of the excitation spectrum is very similar to that of the MLCT absorption of the dye, its maximum being located around 455 nm. The lowest excited state of the $\text{RuL}_2\text{L}'$ is likely to correspond to an electronic configuration, where the electron is predominantly present on one of the two phenanthroline ligands. This is due to the fact that the energy level of the π^* orbital of the diphenylphenanthroline is lower than that of the bipyridine-4,4'-diphosphonate.

Figure 2a shows a current voltage curve obtained with a nanocrystalline TiO_2 film deposited on the titanium rod and coated with a monolayer of $\text{RuL}_2\text{L}'$. The electrolyte was DMF

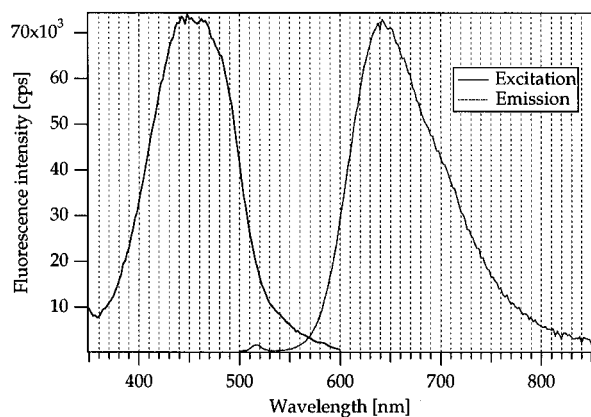


Figure 1. Excitation and emission spectra of a 10^{-6} M solution of $\text{RuL}_2\text{L}'$ in DMF: excitation wavelength, 450 nm; emission wavelength, 642 nm. The absorption matches the excitation spectrum: the maximum is located at 455 nm, the decadic molar extinction coefficient being $\epsilon(455) = 27\,400 \text{ l mol}^{-1} \text{ cm}^{-1}$.

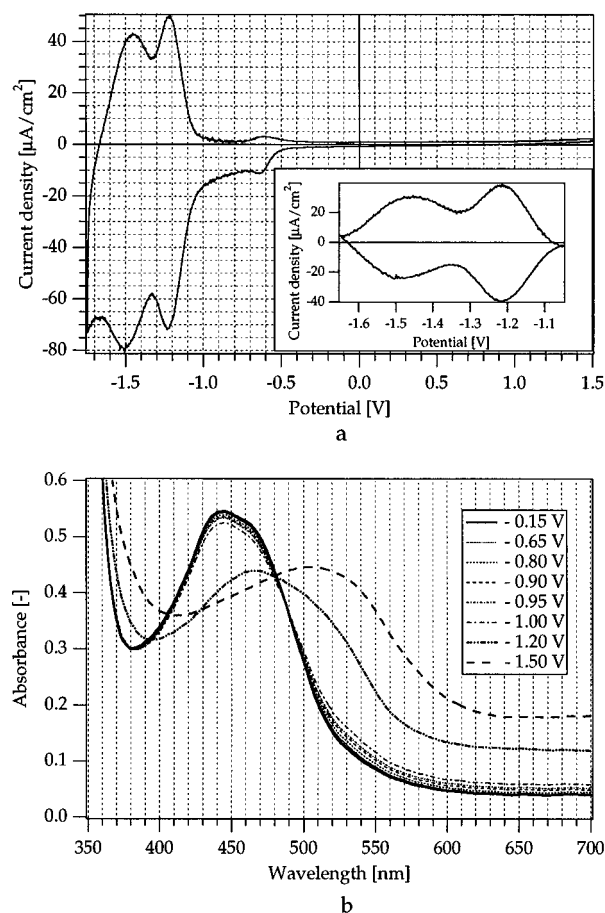


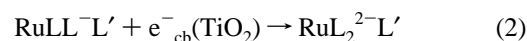
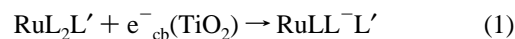
Figure 2. (a) Cyclic voltammety of a TiO_2 electrode coated with $\text{RuL}_2\text{L}'$, the electrolyte being 0.1 M $(\text{TBA})\text{BF}_4$ in DMF (scan rate, 20 mV/s). (b) Effect of applied potential on the absorption in a nanocrystalline TiO_2 layer coated with a monolayer of $\text{RuL}_2\text{L}'$, electrolyte: 0.1 M $(\text{TBA})\text{BF}_4$ in DMF. The data presented are difference spectra, the background absorption of the electrolyte being subtracted from the measured absorption values.

containing 0.1 M $(\text{TBA})\text{BF}_4$. At potentials positive of the flat band potential (V_{fb}), which is estimated to be ≈ -0.5 V where the electrode is under reverse bias, the current is practically zero. (For conventional semiconductors, the flat band potential is defined as the potential at which there is no band bending present in the solid. Negative polarization with respect to V_{fb} results in majority carrier accumulation, while positive polarization leads to their depletion. In the case of the nanocrystalline

TiO_2 films employed here the definition of V_{fb} is problematic because the band bending in the depletion range is small for weakly doped solids.¹² Therefore we shall identify in the following V_{fb} with the potential at which accumulation of majority carriers starts at the interface. In other words at $V < V_{\text{fb}}$ the electrode is under forward bias. An alternative terminology employed for nanocrystalline films is the potential of the conduction band edge at the solid liquid interface V_{cb} . The two potentials are related by the equation¹⁹

$$V_{\text{cb}} = V_{\text{fb}} + kt \ln \frac{[e^-_{\text{cb}}]}{[n_{\text{cb}}]}$$

where $[e^-_{\text{cb}}]$ is the concentration of electrons in the conduction band estimated to be between 10^{16} and 10^{17} cm^{-3} and $[n_{\text{cb}}]$ is the concentration of accessible electronic states in the conduction band, about 4×10^{21} for TiO_2 . Therefore V_{cb} is about 300 mV more negative than V_{fb} . The value of $V_{\text{fb}} \approx -0.5$ V is estimated from the onset of the electroluminescence which coincides with the maximum of the photoluminescence, as will be shown below in Figures 3a and 4a. Under forward bias, a small hump appears first at ca -0.65 V, which is attributed to capacitive charging of the film including filling of surface states and to the reduction of small amounts of titanium peroxides formed inadvertently by band gap excitation of TiO_2 .²⁰ This feature is also observed with blank TiO_2 films in the absence of adsorbed dye. The current voltage curve obtained after deduction of the background current due to the TiO_2 is shown in the inset of Figure 2a. Two pronounced waves are clearly discernible. For the first reduction, the anodic and cathodic peaks are at the same potential, i.e., at -1.22 V, indicating a reversible redox process involving a surface-adsorbed depolarizer. For the second wave the cathodic and anodic peaks are separated by ca. 20 mV, the midpoint potential being -1.49 V. The ratio of areas under the two waves was determined as 1.05, indicating reduction of the surface-anchored $\text{RuL}_2\text{L}'$ by two successive one-electron transfer reactions, i.e.,



Because the two LUMOs of $\text{RuL}_2\text{L}'$ correspond to the diphenylphenanthroline π^* orbitals, the product of the reduction steps are best described as $\text{Ru}(\text{II})$ complexes having one or two unpaired electrons located on the phenanthroline ligands.

This assignment was confirmed by spectro-electrochemical experiments. The absorption spectrum of the nanocrystalline TiO_2 film, loaded with a monolayer of $\text{RuL}_2\text{L}'$ and deposited on a conducting glass electrode, was monitored as a function of electrode potential. Results are shown in Figure 2b, which illustrates the effect of electrode potential on the absorption spectrum of the film. The spectra displayed have been corrected for the extinction of the electrolyte. The absorption of the electrode remained practically unchanged, corresponding to the MLCT transition of $\text{RuL}_2\text{L}'$ in the voltage range positive of the flat-band potential (≈ -0.5 V). Applying a forward bias increases at first slightly the absorption in the red due to the accumulation of conduction band electrons.¹²⁻¹⁴ At more negative potentials, a pronounced red shift in the absorption appears which is clearly associated with the two electrochemical reduction waves shown in Figure 2a. At -1.5 V the absorption maximum is at 520 nm, the spectral features turning into those characteristic for reduced ruthenium-polypyridyl complexes,²¹

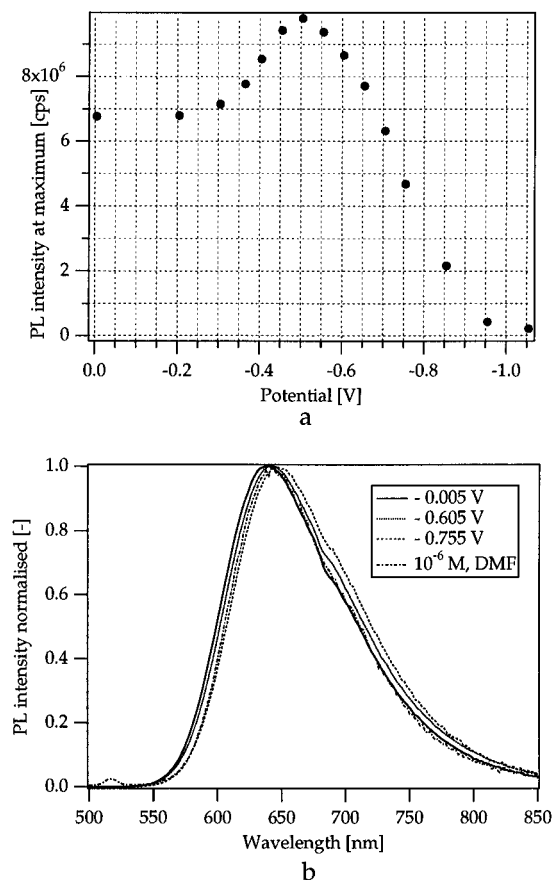


Figure 3. Photoluminescence of $\text{RuL}_2\text{L}'$ deposited on the TiO_2 layer. Electrolyte: 0.1 M (TBA) BF_4 in DMF; excitation wavelength, 448 nm with interference filter. (a) Photoluminescence versus potential: emission wavelength, 632 nm. The measurements have been performed in steady state. (b) Spectra taken at different potentials. The spectrum of a 10^{-6} M solution of the dye in DMF is reported for comparison.

confirming the occurrence of reactions 1 and 2 at the nanocrystalline TiO_2 surface.

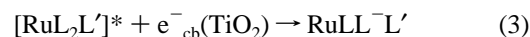
Cyclic voltammetry was also performed with the mesoporous TiO_2 films deposited on conducting glass which due to their larger surface area allow for a more precise determination of the adsorbed quantity of $\text{RuL}_2\text{L}'$ than the titanium rod based electrodes employed in Figure 2a. The adsorbed amount of dye on this particular electrode was calculated as 2.3×10^{-8} mol/ cm^2 from the decrease of the dye concentration in solution measured by transmission spectroscopy. Integrating of the first wave in the cyclic voltammogram and taking the average of the charge passed during the cathodic and anodic part of the redox process gave 2×10^{-8} mol/ cm^2 . Since the graphical integration is not very precise this agreement is satisfactory, indicating that all of the $\text{RuL}_2\text{L}'$ adsorbed on the mesoporous surface is electroactive.

Figure 3a illustrates the effect of the electrode potential on the intensity of the photoluminescence of $\text{RuL}_2\text{L}'$ measured at 632 nm. These experiments employed a 1 cm^2 sized mesoporous TiO_2 film deposited on a titanium plate substrate as a working electrode together with an electrolyte consisting of 0.1 M (TBA) BF_4 in dry DMF. At a potential of 0 V, a significant emission is observed yielding a photon count of 6.8×10^6 s^{-1} at the detector. Applying a negative potential to the electrode enhances first the emission until it reaches a maximum of 9.8×10^6 photons s^{-1} at -0.52 V. Further decreasing the potential leads to a decline of the luminescence intensity, which becomes negligibly small at potentials below -1 V. The electrode potential exerts also a small influence on the emission maximum,

which is red-shifted by about 10 nm upon changing the polarization from 0 to -1 V as shown in Figure 3b. The appearance of this red shift is attributed to the effect of the local electrostatic field on the MLCT electron transition, which changes upon varying the electrode polarization.

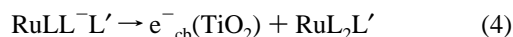
These observations can be rationalized in terms of electron and energy transfer quenching of the excited state of $\text{RuL}_2\text{L}'$ at the TiO_2 surface. Sensitized electron injection from $\text{RuL}_2\text{L}'$ in the conduction band of TiO_2 occurs in the potential domain positive of -0.52 V where the film is under reverse bias. A nanocrystalline photovoltaic cell constructed from a working electrode constituted by a TiO_2 film deposited on a conductive SnO_2 glass and loaded with $\text{RuL}_2\text{L}'$, a conducting glass counter electrode activated with a $5 \mu\text{g}/\text{cm}^2$ Pt catalyst, and a solution of 0.5 M 1-hexyl-3-methylimidazolium iodide and 40 mM iodine in DMF as redox electrolyte yielded a current action spectrum whose features closely resembled those of the $\text{RuL}_2\text{L}'$ absorption spectrum. The injection was highest at 460 nm, where the monochromatic efficiency for photon to current conversion reached 9% under short circuit conditions. The enhancement of the luminescence intensity upon changing the potential from -0.3 to -0.5 V in Figure 3a is due to the decrease of the efficiency of electron injection which competes with photoluminescence. As the electrode potential approaches the flat band value, the electron injection is impaired, decreasing the injection yield and hence enhancing the luminescence. A similar effect was observed earlier¹ with ruthenium tris(2,2'-bipyridine-4,4'-dicarboxylate), whose luminescence was turned on upon approaching the flatband potential of the nanocrystalline TiO_2 film. However, the decline of the emission intensity under forward bias, which is apparent in Figure 3a, was not observed in the earlier study, probably due to desorption of the sensitizer from the electrode under accumulation condition. Such a desorption does not occur in the case of $\text{RuL}_2\text{L}'$, which due to the phosphonate groups remains strongly anchored to the film even after reduction. The intimate association of $\text{RuL}_2\text{L}'$ with the TiO_2 favors energy transfer from the excited sensitizer to conduction band electrons. Because the concentration of the latter is increasing exponentially with applied voltage under forward bias, energy transfer is competing more and more effectively with other deactivation pathways until, at potentials below -0.9 V, it becomes the dominant channel of the $\text{RuL}_2\text{L}'$ excited state reaction.

It should be noted that, apart from energy transfer, there is another pathway for excited state deactivation. It involves the reductive quenching of the excited state of $\text{RuL}_2\text{L}'$ by conduction band electrons to form the reduced state of the complex:



In order to check whether such a mechanism is operative in the present case, we have examined films loaded with $\text{RuL}_2\text{L}'$ by laser photolysis. The $\text{RuL}_2\text{L}'$ was electronically excited by a 532 nm pulse of 10 ns half-width from a frequency-doubled Nd Laser and the time course of the visible absorption monitored by transient optical absorption spectroscopy. It was placed in contact with an electrolyte consisting of 0.1 M (TBA) BF_4 in dry DMF and its potential adjusted to -0.9 V. The changes in the absorbance in the 500 nm region where $\text{RuLL}^-\text{L}'$ has an absorption maximum were monitored following laser excitation. The signal observed was very weak, typically absorbance changes were below 10^{-4} , even though the energy of the exciting laser pulse was as high as 53 mJ. This shows that if any $\text{RuLL}^-\text{L}'$ formed via reaction 3, it remained below detection level and that its yield is therefore very small. One might argue that reaction 3 could be followed by charge injection from the

reduced state of the complex in the TiO₂ conduction band, eq 4, and that this reaction could be so fast that the RuLL⁻L' would



become undetectable on the nanosecond time scale of the laser experiment. While this possibility cannot be totally discarded on the basis of the available evidence, it is unlikely for reaction 4 to happen on a subnanosecond time scale as the accumulation layer field present in the TiO₂ at the applied forward bias impairs charge injection. This effect is clearly visible in Figure 3 and was already discussed in this context.

The efficient quenching of the RuL₂L' luminescence observed under forward bias confirms that the phosphonated ruthenium polypyridyl-type complexes remain strongly anchored to the TiO₂ surface under accumulation conditions, in agreement with the electrochemical results shown above. Only if during accumulation the ruthenium complex remains in close proximity to the semiconductor solid can the excited state deactivation take place so efficiently. Similar observations have been made very recently by Yan and Hupp²² with the phosphonated bipyridyl complex RuL₃, where L stands for 4,4'-H₂O₃PCH₂-2,2'-bipyridine which was also anchored to the surface of a mesoporous TiO₂ film. Under forward bias a very rapid excited state deactivation was observed which was tentatively attributed to energy transfer quenching by conduction band electrons. The existence of such a quenching mode has important consequences for reactions involving excited states at semiconductor electrodes. In general, it constitutes a loss channel, reducing the yield of the competing desirable excited state reaction.

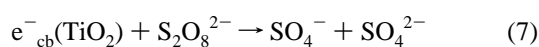
Figure 4a shows the electroluminescence obtained with RuL₂L' as a sensitizer using a nanocrystalline TiO₂ film for electron injection. The corresponding current voltage curve is also shown on this picture. The working electrode was a titanium rod covered with the mesoporous TiO₂ together with an electrolyte consisting of 0.1 M (TBA)BF₄ and 5 mM Na₂S₂O₈ in dry DMF. A cathodic current due to the reduction of peroxydisulfate appears at potentials negative of the flat band potential (≈ -0.5 V). Electroluminescence is produced concomitantly with the flow of cathodic current across the interface. The emission intensity is strongly enhanced by increasing the forward bias, and this is associated with a steep rise in the cathodic current due to the reduction of peroxydisulfate. The spectral distribution of the emission shown in Figure 4b matches well the features of the photoemission of RuL₂L' presented by the solid line. This confirms that the electroluminescence arises from the excited state of RuL₂L' and not from the TiO₂. The emission originates from electron injection from the conduction band of the TiO₂ film into the π* orbital of the phenanthroline ligand of [RuL₂L']⁺, generating the lowest excited state of the ruthenium complex which is the light emitting species.



[RuL₂L']⁺ is generated via reaction of the sensitizer with sulfate radical ion which is a strong oxidant (*E*⁰ = +2.43 (vs SCE) in water)²³



the latter being generated through the reduction of peroxydisulfate with conduction band electrons:



This excited state production can be visualized as the removal

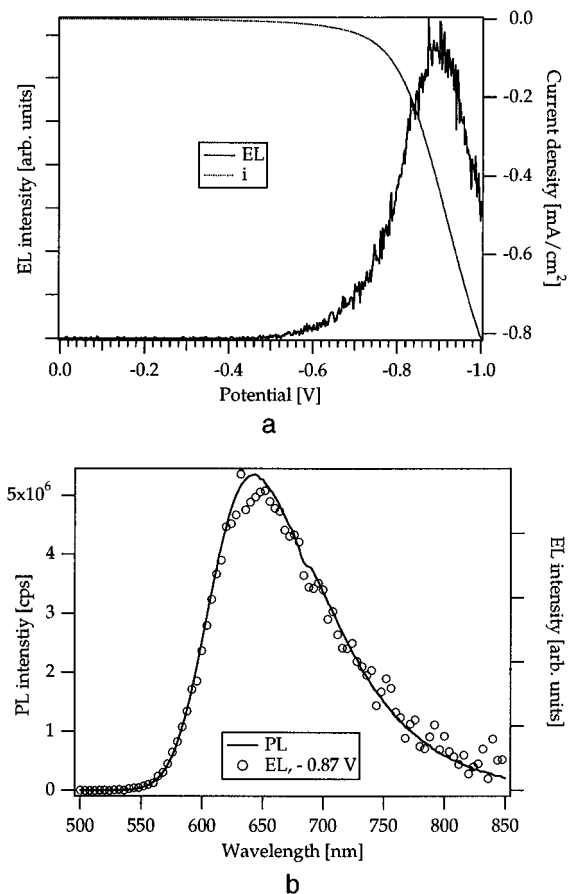


Figure 4. Electroluminescence of RuL₂L' deposited on the TiO₂ layer (electrolyte: 5 mM Na₂S₂O₈, 0.1 M (TBA)BF₄ in DMF): rotation rate, 1000 rpm. (a) Dependence of the EL vs potential: scan rate, 2 mV/s; emission wavelength, 640 nm. (b) Spectrum taken at a pulsed potential: -0.17 V/900 ms, -0.87 V/100 ms. The photoluminescence spectrum in the same electrolyte is reported for comparison (excitation wavelength, 448 nm with interference filter, TiO₂ layer deposited on a Ti plate).

of an electron from the Ru(II) metal center, yielding the trivalent ruthenium complex followed by the addition of an electron to one of the phenanthroline ligands. The resulting electronic configuration where one electron is missing in the HOMO while the LUMO is occupied by one electron corresponds to that of the MLCT excited state of RuL₂L'.

The presence of a maximum in the electroluminescence intensity in Figure 4a is expected since the conduction band electrons necessary for the generation of excited states act also as quenchers for the same states. Sweeping the voltage negative of the flat-band potential enhances the rate of excited state production via reaction 5–7. At the same time the quenching rate of the excited state by energy transfer is enhanced since the concentration of the conduction band electrons augments with increasing forward bias. Hence, there is an optimum potential situated around -0.88 V. The position of this maximum remained approximately constant under repeated scanning. However, a marked reduction in both the cathodic current and the electroluminescence was observed when the potential of the electrode was cycled between 0 and -1 V. This effect presumably arises from a side reaction of the persulfate leading to oxidation of DMF under formation of a passivating layer at the TiO₂ surface.

The present study shows that electroluminescence can be produced via electron injection from the conduction band of a semiconducting oxide into the oxidized state of a surface adsorbed sensitizer, producing directly its light emitting elec-

tronic state. An alternative mechanism for which the term electrogenerated chemiluminescence has been coined^{24,25} is often operative in the case of metallic electrodes. Here, the oxidized and reduced form of sensitizer is produced electrochemically and light is generated when the two species react to give back two sensitizer molecules in their original oxidation state. It involves reduction of the RuL₂L' by conduction band electrons generating RuLL⁻L' followed by the reaction of the latter with the oxidized complex [RuL₂L']⁺ to produce the excited state of the complex. In the present case, direct electron injection from the nanocrystalline oxide to the oxidized sensitizer is the dominant pathway by which electroluminescence is generated. This is clearly apparent from the fact that the onset of the luminescence is at a voltage sufficiently negative to produce the excited state directly via reaction 5 but insufficient to reduce the ground state complex according to eq 1. Recall that the electroluminescence rises at potentials more negative than -0.5 V, whereas the thermodynamical potential of the first reduction for RuL₂L' is at -1.22 V. Moreover, it is well-established²⁶ that the redox potential for the oxidation of the excited state of polypyridyl-ruthenium(II) complexes is about 0.5 V more positive than the ground state reduction potential of the same complexes. Thus, while the production of an excited state through electron transfer into the LUMO of the Ru(III) complex at potential of -0.5 V is possible, the reduction of the ground state complex does not occur at this potential.

Only four previous examples of electroluminescence induced by direct heterogeneous electron transfer from a semiconductor electrode to the oxidized state of a dye are known, but, in those cases, the dyes were dissolved in solution and not adsorbed at the semiconductor surface. The reduction of Ru(bpy)₃³⁺ by an electron from the conduction band of SiC or GaP electrode leads partially to the formation of [Ru(bpy)₃²⁺]^{*} which emits light.²⁷ The reduction of the rubrene radical cation by an electron from the conduction band of a ZnO or CdS electrode leads partially to the formation of the triplet excited state of rubrene.^{28,29} Two triplet excited states annihilate to form one rubrene molecule in the ground state and another one in the singlet excited state which emits light.

Conclusion

For the first time, the production of an excited state by heterogeneous electron transfer from the conduction band of a nanocrystalline TiO₂ electrode into the π* level of an oxidized polypyridyl-ruthenium(II) complex which is grafted on the surface of the oxide has been demonstrated. The morphology of the electrode plays an important role in favoring the electroluminescent process. The high surface area of such an electrode allows a decrease of the electron density in the conduction band compared to a flat electrode, maintaining the high current intensity based on the projected surface area. The high internal surface area not only permits a decrease in the

overpotential necessary to drive the electron transfer but also allows a dramatic decline of the quenching rate of the excited state by energy transfer to free electrons in the conduction band. Therefore, one can be confident that these films will play an important role in the design of future electroluminescent devices.

Acknowledgment. Support of this work by a grant from the Swiss National Science Foundation and by the Optics Priority Program of the Swiss Confederation is gratefully acknowledged. The authors are grateful to Dr. Robin Humphry-Baker for assistance in the laser experiment and for helpful discussions.

References and Notes

- O'Regan, B.; Moser, J.; Anderson, M.; Grätzel, M. *J. Phys. Chem.* **1990**, *94*, 8720.
- Hagfeldt, A.; Björkstén, U.; Lindquist, S.-E. *Sol. Energy Mater. Sol. Cells* **1992**, *27*, 293.
- Hodes, G.; Howell, I. D. J.; Peter, L. M. *J. Electrochem. Soc.* **1992**, *139*, 3136.
- Liu, D.; Kamat, P. V. *J. Phys. Chem.* **1993**, *97*, 10769.
- Hoyer, P.; Eichberger, R.; Weller, H. *Ber. Bunsen-Ges. Phys. Chem.* **1993**, *97*, 630.
- Meyer, G. J.; Searson, P. C. *Electrochem. Soc. Interface* **1993**, *2*, 23.
- Konenkamp, R.; Henninger, R. *Appl. Phys. A* **1994**, *58*, 87.
- O'Regan, B.; Grätzel, M. *Nature* **1991**, *353*, 737.
- Nazeeruddin, M. K.; Kay, A.; Rodicio, L.; Humphry-Baker, R.; Müller, E.; Liska, P.; Vlachopoulos, N.; Grätzel, M. *J. Am. Chem. Soc.* **1993**, *115*, 6382.
- Knodler, R.; Sopka, J.; Harbach, F.; Grunling, H. W. *Sol. Energy Mater. Sol. Cells* **1993**, *30*, 277.
- Hagfeldt, A.; Didriksson, B.; Palmqvist, T.; Lindstrom, H.; Sodergren, S.; Rensmo, H.; Lindquist, S. E. *Sol. Energy Mater. Sol. Cells* **1994**, *31*, 481.
- Rothenberger, G.; Fitzmaurice, D.; Grätzel, M. *J. Phys. Chem.* **1992**, *96*, 5983.
- Redmond, G.; Fitzmaurice, D. *J. Phys. Chem.* **1993**, *97*, 1426.
- Redmond, G.; Okeeffe, A.; Burgess, C.; Machale, C.; Fitzmaurice, D. *J. Phys. Chem.* **1993**, *97*, 11081.
- Björkstén, U.; Moser, J.; Grätzel, M. *Chem. Mater.* **1994**, *6*, 858.
- Hirao, T.; Masunaga, T.; Ohshiro, Y.; Agawa, T. *Synthesis* **1981**, 56.
- Maerker, G.; Case, F. H. *J. Am. Chem. Soc.* **1958**, *80*, 2745.
- Bonhôte, P.; Dias, A. P.; Papageorgiou, N.; Kalyanasundaram, K.; Grätzel, M. *Inorg. Chem.* **1996**, *35*, 1168.
- O'Regan, B.; Moser, J.; Anderson, M.; Grätzel, M. *J. Phys. Chem.* **1990**, *94*, 8720.
- Augustynski, J. *Struct. Bonding* **1988**, *69*, 1.
- Kalyanasundaram, K. *Photochemistry of Polypyridine and Porphyrin Complexes*; Academic Press, Ed.; Harcourt, Brace, Jovanovich: London, 1992, p 636.
- Yan, S. G.; Hupp, J. T. *J. Phys. Chem.* **1996**, *100*, 6867.
- Huie, R. E.; Clifton, C. L.; Neta, P. *Radiat. Phys. Chem.* **1991**, *38*, 477.
- Laser, D.; Bard, A. J. *J. Electrochem. Soc.* **1975**, *122*, 632.
- Xu, X. H.; Shreder, K.; Iverson, B. L.; Bard, A. J. *J. Am. Chem. Soc.* **1996**, *118*, 3656.
- Juris, A.; Balzani, V.; Barigelletti, F.; Campagna, S.; Belser, P.; von Zelewsky, A. *Coord. Chem. Rev.* **1988**, *84*, 85.
- Gleria, M.; Memming, R. *Z. Phys. Chem.* **1976**, *101*, 171.
- Yeh, L.-S. R.; Bard, A. J. *Chem. Phys. Lett.* **1976**, *44*, 339.
- Luttmer, J. D.; Bard, A. J. *J. Electrochem. Soc.* **1978**, *125*, 1423.